J Mater Sci: Mater Med (2009) 20:1729–1741
DOI 10.1007/s10856-009-3722-4

Microporous biodegradable polyurethane membranes for tissue engineering

Yuen Kee Tsui · Sylwester Gogolewski

Received: 4 October 2008 / Accepted: 23 February 2009 / Published online: 20 March 2009

Abstract Microporous membranes with controlled pore size and structure were produced from biodegradable polyurethane based on aliphatic diisocyanate, poly(ε-caprolactone) diol and isosorbide chain extender using the modified phase-inversion technique. The following parameters affecting the process of membrane formation were investigated: the type of solvent, solvent–nonsolvent ratio, polymer concentration in solution, polymer solidification time, and the thickness of the polymer solution layer cast on a substrate. The experimental systems evaluated were polymer–*N*,*N*-dimethylformamide–water, polymer–*N*,*N*-dimethylacetamide–water and polymer–dimethylsulfoxide–water. From all three systems evaluated the best results were obtained for the system polymer–*N*,*N*-dimethylformamide–water. The optimal conditions for the preparation of microporous polyurethane membranes were: polymer concentration in solution 5% (w/v), the amount of nonsolvent 10% (v/v), the cast temperature 23°C, and polymer solidification time in the range of 24–48 h depending on the thickness of the cast polymer solution layer. Membranes obtained under these conditions had interconnected pores, well defined pore size and structure, good water permeability and satisfactory mechanical properties to allow for suturing. Potential applications of these membranes are skin wound cover and, in combination with autogenous chondrocytes, as an "artificial periosteum" in the treatment of articular cartilage defects.

Various parts of this study were presented at the European Society for Biomaterials Meeting, Sorrento, Italy, September 11–15, 2005, and at the International Conference on Advanced Materials Design & Development (ICAMDD 2005), Goa, India, December 14–16, 2005. An experimental part of this work was carried out at the Polymer Research Department, AO Research Institute, Clavadelerstrasse 8, CH-7270 Davos, Switzerland.

Y. K. Tsui
Department of Orthopaedics and Traumatology, The University of Hong Kong, 21 Sassoon Road, Pokfulam, Hong Kong, SAR

S. Gogolewski (✉)
Department of Biomedical Engineering, University of Zielona Gora, Podgorna 50, Zielona Gora 65-246, Poland
e-mail: sylwester.gogolewski@neostrada.pl;
S.Gogolewski@ibem.uz.zgora.pl

1 Introduction

Interest in biodegradable polyurethanes for implantable devices goes back to the early 1980s [1–12]. Continuing efforts to replace defective tissues and organs using tissue engineering approaches [13] have been the reason that interest in biodegradable polyurethanes has gained new momentum [14–36]. The numerous possible applications for biodegradable polyurethanes in tissue engineering include use as three-dimensional porous scaffolds for cancellous bone graft substitutes and microporous membranes for the treatment of articular cartilage defects in procedures where cultured autogenous chondrocytes are applied in combination with an autogenous periosteal flap [37, 38]. As harvesting a periosteal flap creates new wounds, the use of an "artificial flap" might not only avoided this problem but also simplify the surgical procedure. In addition such flaps could be seeded with autogenous chondrocytes to facilitate defect healing. Microporous membranes from elastomeric biodegradable polyurethanes are among the candidates for such artificial periosteal flaps.

There are various techniques available to produce porous polymeric structures. These include solvent casting-

particulate leaching, gas foaming, freeze drying, electrostatic spinning, solid free form fabrication, and phase-inversion, to mention but a few [39–47]. Phase inversion is a process whereby a polymer is transformed in a controlled manner from a liquid to a solid state. Phase-inversion can be initiated by solvent evaporation, thermal precipitation or precipitation with nonsolvent, the latter being especially well suited for the fabrication of microporous polymeric membranes. In this process, interdiffusion of the solvent with the nonsolvent results in the decomposition of polymer solution into a polymer-rich phase and a polymer-poor phase. Consequently, the polymer-rich phase is solidified into a solid matrix, while the polymer-poor phase forms the pores. Depending on the conditions of phase-inversion the porous polymeric structures formed will differ in pore size, geometry, distribution and interconnectivity. Pore interconnectivity facilitating the flux of nutrients, cell proliferation and vascularization is particularly important when porous structures are used as scaffolds for tissue engineering.

This study addresses the design of biodegradable microporous polyurethane membranes for tissue engineering using the modified phase-inverse technique. Potential applications of the membranes are as "periosteal flaps" in the treatment of articular cartilage defects and as skin wound covers.

2 Experimental

2.1 Biodegradable polyurethane

The biodegradable polyurethane with a number-average molecular weight of 224,900 Da and a weight-average molecular weight of 509,700 Da used in this study was synthesized using hexamethylene diisocyanate, poly(ε-caprolactone) MW = 530 Da and isosorbide chain extender. Details of the polymer synthesis have been given elsewhere [14, 15]. The as-synthesized polyurethane was purified by dissolution in DMF, filtration through a S-2 sintered glass filter followed by precipitation with ethanol-distilled water mixture (1:3) to remove oligomeric fractions [15]. Subsequently, the polymer was dried at 60°C under vacuum for at least 24 h and stored in a desiccator prior to use.

2.2 Preparation of polymer solutions

The dry polyurethane was dissolved in *N*,*N*-dimethylformamide (DMF), *N*,*N*-dimethylacetamide (DMAC) and dimethylsulfoxide (DMSO) (Fluka Chemie GmbH, Buchs, Switzerland) to obtain solutions with the required concentration (%, w/v) and filtered through S-2 sintered glass filters. All solutions were kept in closed Erlenmeyer flasks to avoid solvent evaporation and water sorption.

2.3 Preparation of membranes

The polymer was dissolved separately in individual solvents and all the membranes were cast from freshly prepared solutions only. Deionized water was used as a nonsolvent (coagulant) and poly(vinyl pyrrolidone) (PVP) (MW = 10,000 Da), poly(ethylene glycol) (PEG) (MW = 2000 Da), sodium carboxymethylcellulose and calcium L-lactate were used as solid porogenes. The porogenes were used separately. All chemicals (Fluka Chemie GmbH, Buchs, Switzerland) were used as received. For the preparation of membranes a predetermined amount of polymer solution in a given solvent was pipetted into Erlenmeyer flasks and then the given amount of nonsolvent and/or solid porogene was added to the polymer solution. The mixture was stirred vigorously in stoppered flasks for 5 h and then poured on Petri-dishes (Ø = 110 mm). Three samples were prepared for each kind of membrane. The polymer was allowed to solidify at 22°C for a given time and then deionized water was poured over the nascent solid polymer gel layer. The system was kept under these conditions until the membrane separated completely from the Petri dish. The time after which the membranes detached from the Petri dish without applying an additional force varied from 1 to 5 min. At this time fresh distilled water was poured into the Petri dish and replaced several times. Next, the membranes were washed in distilled water to remove solvent residues and consecutively rinsed with ethanol. The membranes were dried at room temperature for 5 days and subsequently in a vacuum oven at 50°C and 2×10^{-1} mbar to a constant weight. In a separate set of experiments the surface of the coagulated polymer gel layer was sprayed with water under pressure of 2 bars. Water was sprayed through a sieve mask (mesh size = 0.04 mm) to produce small droplets of uniform size. The purpose of this experiment was to assess whether such treatment contributed to the structure and size of pores formed at the surface layer. The parameters varied were polymer concentration in a given solvent, the amount of nonsolvent, the type and amount of a solid additive, the thickness of cast polymer solution layer and the time allowed for coagulation. The effect of polymer concentration on the membranes' properties was investigated for solutions in DMF. The polymer concentrations were 2.5%, 5%, and 10% (w/v). The experimental conditions for preparation of membranes are listed in Table 1, and a simplified scheme of the technique is shown in Fig. 1.

Table 1 Experimental conditions for the preparation of microporous polyurethane membranes

Experiment	Membrane index	Solvent	Solvent evaporation time (h)	Thickness of cast solution layer (mm)	Polymer concentration (w/v)
Effect of solvent type	PU-DMF	DMF	24	1	5%
	PU-DMSO	DMSO	24	1	5%
	PU-DMAC	DMAC	24	1	5%
Effect of liquids evaporation time	PU-DMF-8 h	DMF	8	1	5%
	PU-DMF-24 h	DMF	24	1	5%
	PU-DMF-48 h	DMF	48	1	5%
	PU-DMF-72 h	DMF	72	1	5%
	PU-DMF-120 h	DMF	120	1	5%
Effect of solution layer thickness	PU-1 mm	DMF	24	1	5%
	PU-2 mm	DMF	24	2	5%
	PU-3 mm	DMF	24	3	5%
Effect of polymer concentration	PU-2.5%	DMF	24	1	2.5%
	PU-5%	DMF	24	1	5%
	PU-10%	DMF	24	1	10%
Polymer solution contains nonsolvent	PU-NS	DMF + H_2O	24	1	5%

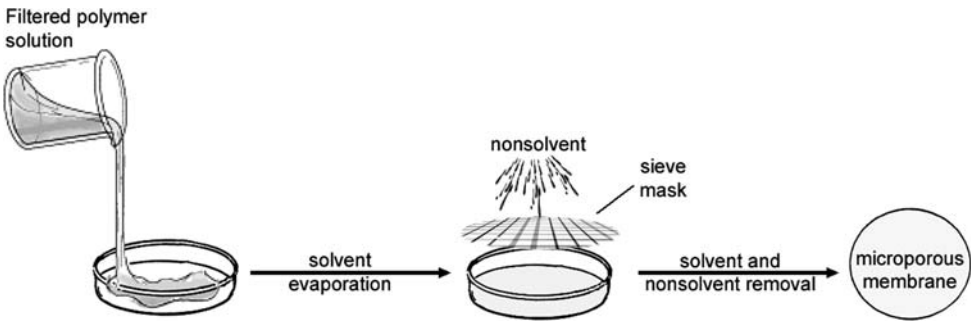

Fig. 1 Simplified view of the membrane preparation procedure

3 Characterization of polyurethane membranes

3.1 Membrane pore size and structure

The porous structure of the polyurethane membranes (glass-contacting surface, air-contacting surface and cross-section) was examined using a scanning electron microscope (Hitachi model S-4100, Tokyo, Japan) operated at 5.0 kV. The cross-sections were produced by slicing the membranes perpendicularly to the glass and the air surfaces into 2 mm sections. Samples (disks with a diameter of 8 mm and cross-sections) were sputtered with 15 nm thick gold–palladium layer. The pore dimension was estimated in two directions, the smallest and the largest.

3.2 Membrane permeability

The water permeability of the polyurethane membranes was measured using a permeation apparatus (Merck, Darmstadt, Germany). Disks with a diameter of 8 mm cut from the membranes were placed in the glass column between two plastic fixtures and the flow rate of water passing through the scaffolds was recorded. Hydrostatic pressure was kept constant during measurement. A stable flux of water through the membranes was obtained after 30 min of operation and the duration of a single measurement did not exceed 20 min. The data presented are the means of six measurements (six samples of each membrane type).

3.3 Thermal analysis

A Perkin-Elmer Pyris DSC-1 differential scanning calorimeter (Norwalk, Connecticut, USA) calibrated with indium was used for the evaluation of the thermal characteristics of the samples. The measurements were carried out under dry, oxygen free nitrogen flowing at a rate of 50–60 ml/min to protect the materials from degradation. The

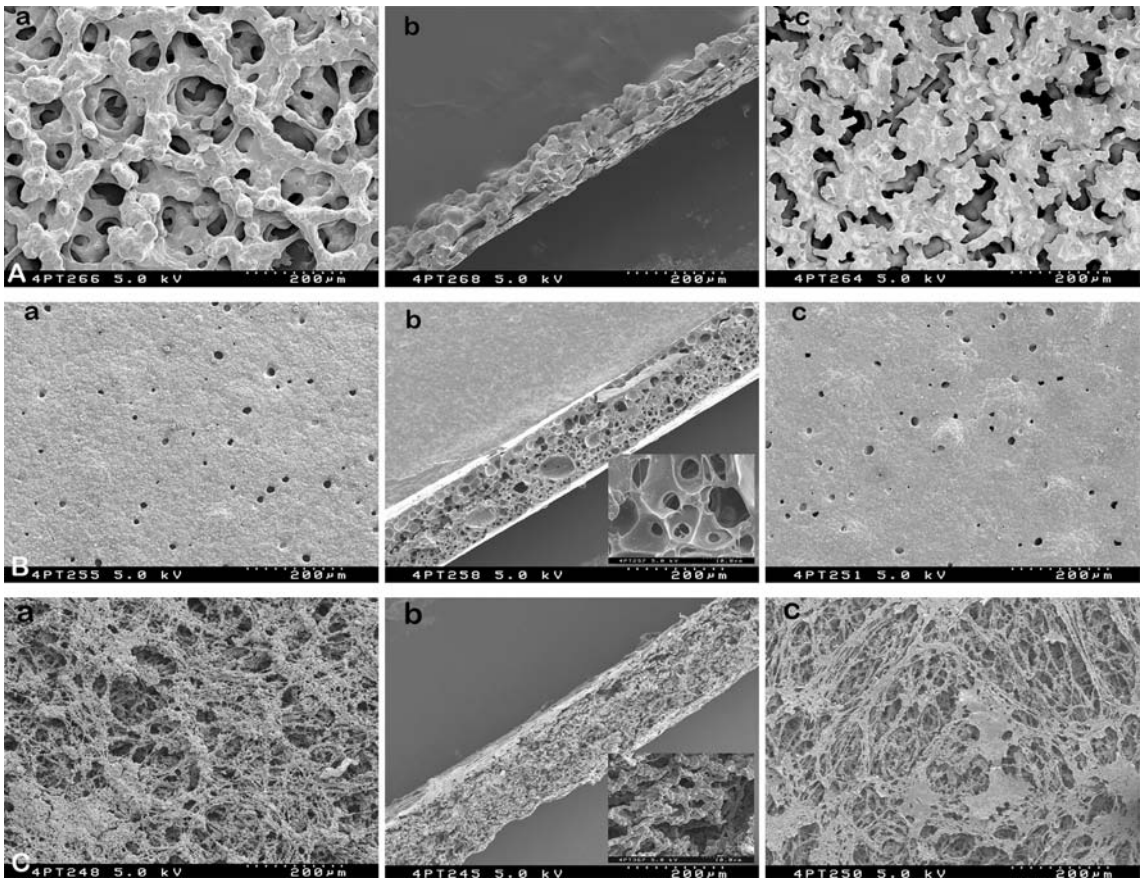

Fig. 2 SEM images of the membranes illustrating the effects of solvent type on the porous structure. The membranes were formed from the 5% (w/v) polyurethane solutions in: **A** DMF; **B** DMSO; and **C** DMAC. The air-contacting surface, the cross-section and the glass-contacting surface are denominated with a, b and c, respectively

weight of samples was in the range of 3–12 mg, the heating rate was 10°C/min and the samples were scanned over a temperature range of 15–250°C. Three samples of each material were used in analysis.

3.4 Mechanical properties

Tensile strengths and Young's moduli of the membranes were measured with an Instron tester model 4302 (High Wycombe, Bucks, England) equipped with a 0.1 kN load cell operating at a cross-head speed of 10 mm/min. The test samples were Type V tensile bars (ASTM D638) cut to shape using a Hollow Die Punch (Model 6051.000, Ceast, Italy). The samples were fixed on the Instron tester using pneumatic-action grips. Suture pull-out strength [48] was measured at a cross-head speed of 12.7 mm/min. Dermalon^{TM} 5.0 nylon monofilament sutures (Tyco Healthcare Group LP, USA) were used in all tests. The quantitative data presented are means of 3 measurements ± standard deviation. The unpaired Student's *t*-test was used for statistical analysis.

4 Results

4.1 Porous structure of membranes

The SEM micrographs illustrating the porous structure of the polyurethane membranes prepared in the present study is shown in (Figs. 2, 3, 4, 5). This structure was dependent on a number of factors including the solvent used for polymer dissolution, the polymer concentration in solution, the presence of nonsolvent, the thickness of polymer solution layer cast on the substrate and the polymer solidification time (the time until the nascent solid polymer gel layer was formed).

4.2 Solvent effect

The surfaces and cross-sections of the membranes formed from the polyurethane solutions in DMF, DMSO and DMAC are shown in Fig. 2. The structure of membranes obtained from the polyurethane solution in DMF (PU-DMF) consisted of thick fibrillar elements. The membranes

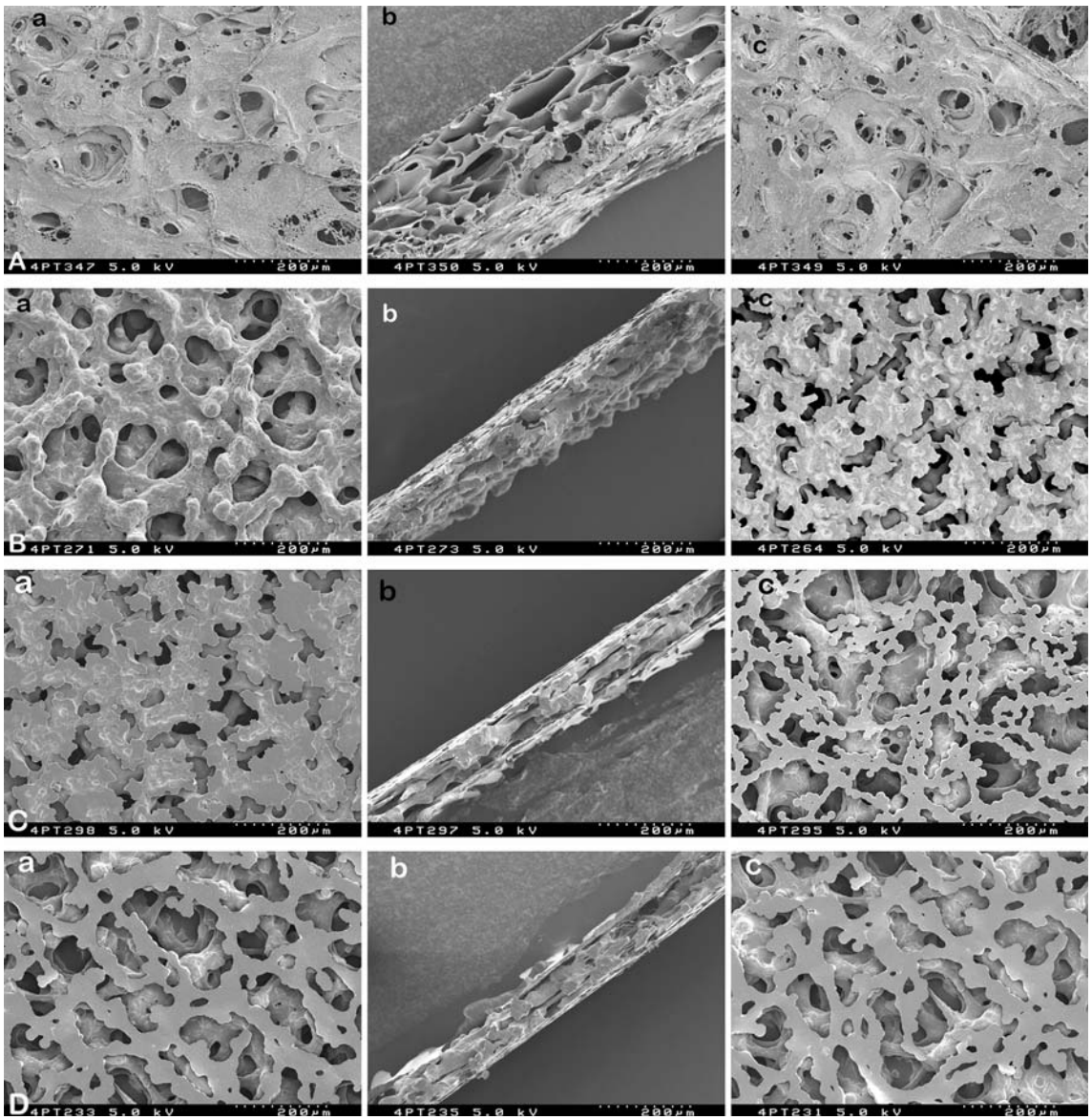

Fig. 3 SEM images of the membranes illustrating the effects of setting time on the porous structure of the membranes formed from the 5% (w/v) polyurethane solutions in DMF. **A** 8 h; **B** 48 h; **C** 72 h; **D** 120 h. SEM images of the membrane formed after 24 h of setting are shown in Fig. 2A. The air-contacting surface, the cross-section and the glass-contacting surface are denominated with a, b and c, respectively

had an interconnected open-pore structure on both surfaces, i.e. the surface in contact with the glass and the surface in contact with the air. Elongated, irregularly shaped pores were randomly distributed in the membrane cross-section. The membranes formed from the polyurethane solution in DMSO (PU-DMSO) had isolated pores with an average size of approximately 5–10 μm on both surfaces and irregular circular pores with sizes in the range of 2–80 μm in the membrane cross-sections. The porous structure of the membranes formed from polymer solution in DMAC (PU-DMAC), consisted of an interconnected network of globules and nodules having no preferential orientation. The pore sizes on both surfaces of the membranes varied from 10 to 200 μm. The pore sizes in the cross-section were in the range of 1–5 μm. On the surface of the membrane in contact with the glass there were flat polymer elements randomly attached to the fibrous structure.

4.3 Polymer solidification time

The term 'solidification time' was defined as the time period until the nascent cast polymer gel layer was covered with a coagulant. The effect of polymer solidification time on the membranes' properties was investigated for the

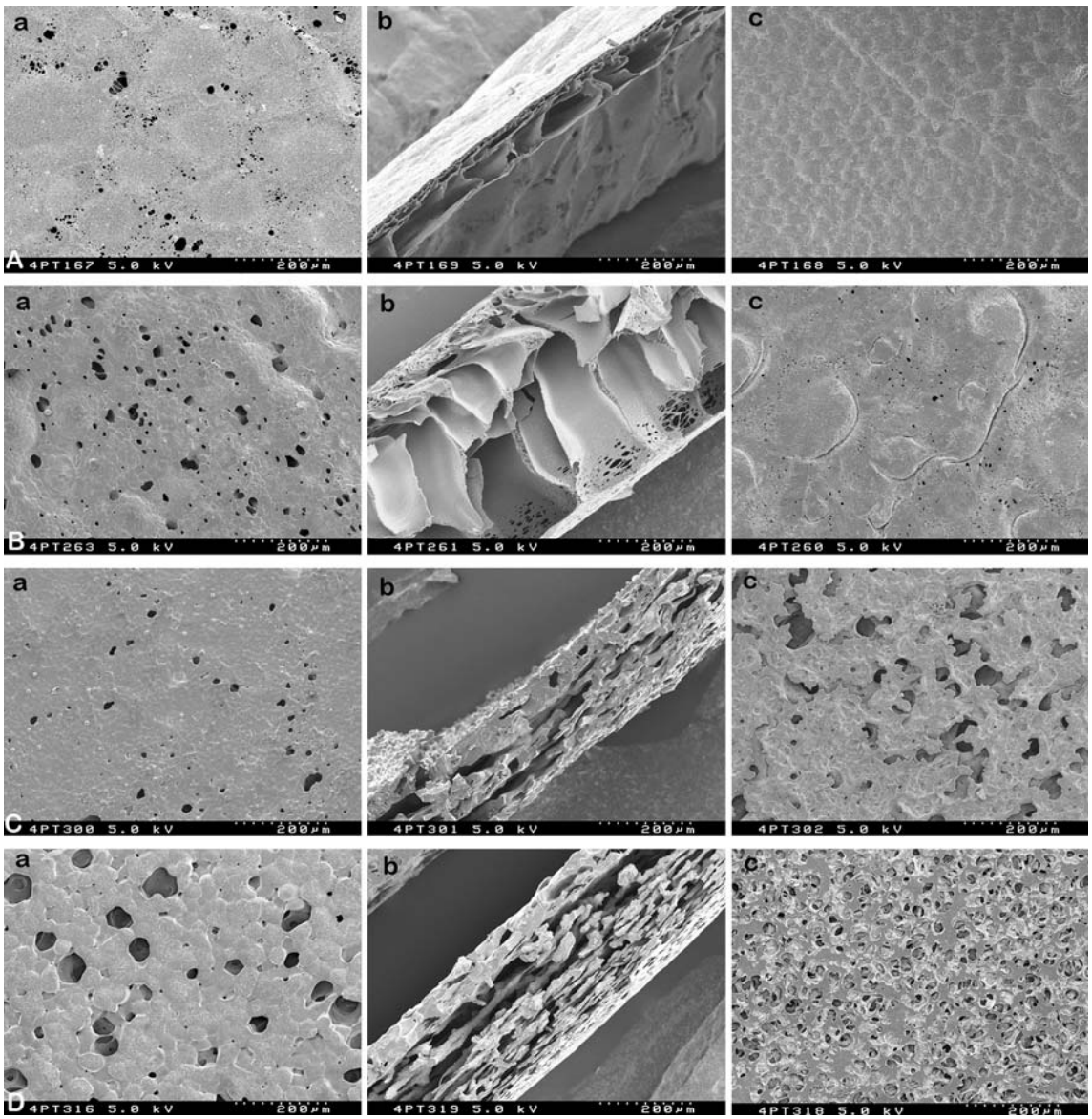

Fig. 4 SEM images of the membranes illustrating the effects of polymer concentration and cast solution layer thickness on the porous structure of the membranes formed from the polyurethane solutions in DMF. **A** 2.5% (w/v); **B** 10% (w/v). The SEM images of the membrane formed from 5% (w/v) solution are shown in Fig. 2A. **C** and **D** illustrate the effect of cast solution layer thickness on the porous structure. **C** 2 mm; **D** 3 mm. SEM images of the membranes formed from 1 mm thick cast solution layer are shown in Fig. 2A. The air-contacting surface, the cross-section and the glass-contacting surface are denominated with a, b and c, respectively

polymer solutions in DMF only as from all three solvents used this solvent provided best results. The polymer concentration in solution was 5% (w/v) and the polymer solidification times were 8, 24, 48, 72 and 120 h. It has been found that irrespective of the solidification time all the membranes had homogenous pore morphology (Fig. 3). The sizes of pores formed in the cross-sections of the PU-DMF-8 h membranes were in the range of 100–150 µm. These pores were separated from each other by microporous walls. The pores on the surfaces of the PU-DMF-8 h membranes were densely packed. There was no evident difference in the pore structure for the membranes cast for 24–120 h. The pores on the surfaces of the PU-DMF-24 h membranes were loosely distributed and the structure of interconnected pores on the surfaces of the PU-DMF-48 h, PU-DMF-72 h and PU-DMF-120 h membranes were comparable. The cross-sections of these membranes seemed to be composed of stacks of separate layers. While the uppermost layer of the of the membrane which solidified for 8 h was highly porous, the cross-sections of the membranes which solidified for 24, 42, 72 and 120 h were practically nonporous. Prolongation of the solidification time led to membranes with more compact polymer layers in the cross-sections. The solidification time also affected

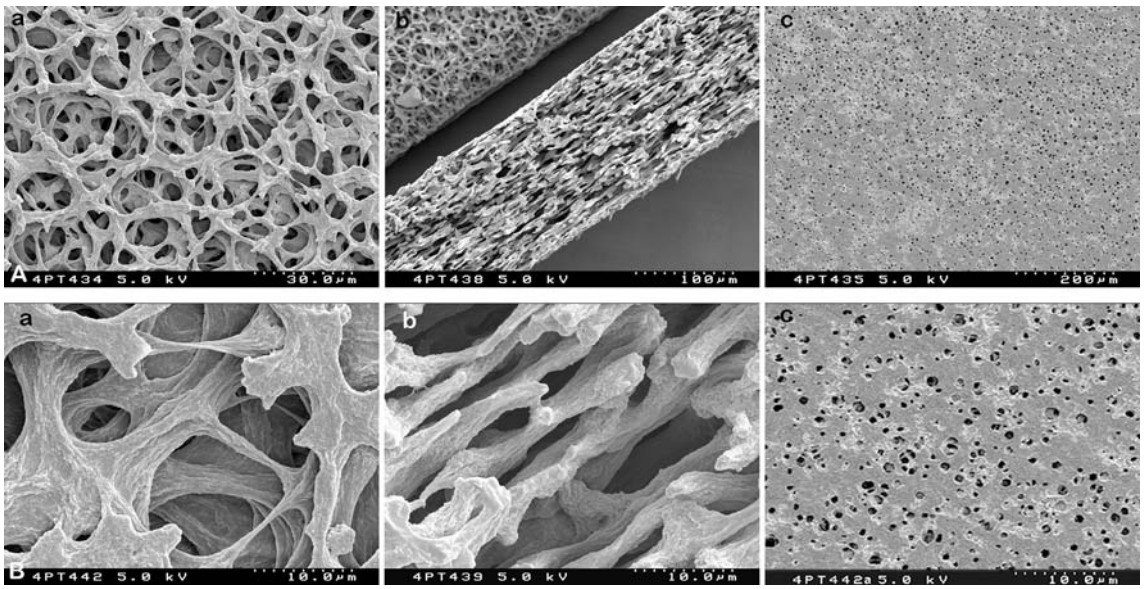

Fig. 5 **A** SEM images of the PU-NS membranes formed from the 5% (w/v) polyurethane solution in DMF containing water as a nonsolvent. **B** SEM images of the PU-NS membranes showed in **A** taken at higher magnification showing the details of the structure. The air-contacting surface, the cross-section and the glass-contacting surface are denominated with a, b and c, respectively

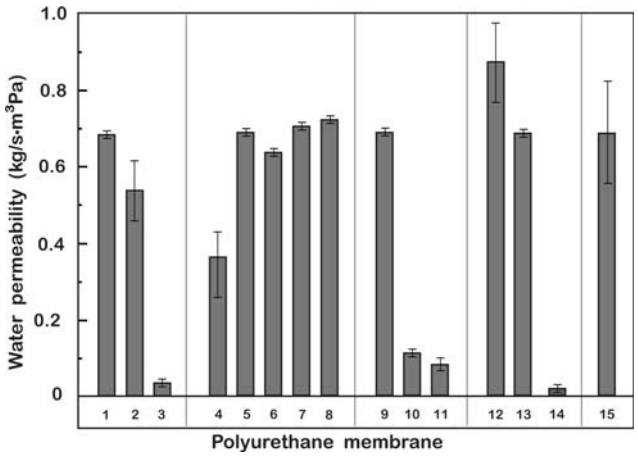

Fig. 6 Water permeability of the porous polyurethane membranes prepared under various experimental conditions. 1. PU-DMF; 2. PU-DMAC; 3. PU-DMSO; 4. PU-DMF-8 h; 5. PU-DMF-24 h; 6. PU-DMF-48 h; 7. PU-DMF-72 h; 8. PU-DMF-120 h; 9. PU-1 mm; 10. PU-2 mm; 11. PU-3 mm; 12. PU-2.5%; 13. PU-5%; 14. PU-10%; 15. PU-NS

the average thicknesses of the membranes. These were 200 µm for the membranes set for 8 h (PU-DMF-8 h) and 100 µm for the membranes set for 24, 48, 72 and 120 h (PU-DMF-24 h, PU-DMF-48 h, PU-DMF-72 h, and PU-DMF-120 h).

4.4 Polymer concentration in solution

The SEM images of the porous structures of the membranes obtained from the polyurethane solutions at concentrations of 2.5%, 5% and 10% (w/v) in DMF (PU-2.5%, PU-5%, PU-10%) are shown in Fig. 4A, B.

The surfaces of PU-2.5% membranes exhibited randomly scattered irregular pinhole-like pores with sizes in the range of 2–25 µm. The air surface of the membranes at higher magnifications showed the presence of pores with sizes in the range of 2–15 µm. In the cross-section of these membranes there were two distinct porous layers varying in thickness. The thinner layer had irregularly shaped pores with an average size in the range of 2–5 µm. The thicker layer had more regularly shaped pores separated by thin walls. The pore sizes in this layer were in the range of 150–200 µm.

The PU-5% membranes had an interconnected open-pore structure consisting of thick fibrillar elements on both surfaces. The membranes' cross-section showed the presence of randomly distributed, irregularly shaped elongated pores.

The PU-10% membranes exhibited a typical palisade-like porous structure with pores aligned perpendicularly to the membrane surfaces. Abundant micropores were present in the walls of the large palisade-like pores. The walls of these micropores with sizes in the range of 1–5 µm consisted of a densely interconnected fibrous network. The surfaces of these membranes were, however, nonporous.

4.5 Thickness of the cast solution layer

In these experiments the thicknesses of cast polymer solution layers were 1, 2, and 3 ± 0.3 mm, respectively. The concentration of polymer solution in DMF was 5% (w/

v). The structure of the resulting microporous membranes is illustrated by SEM micrographs Fig. 4C, D. As it might be expected, the thickness of the membranes increased with increasing thickness of the cast polymer solution layer. The surfaces of membranes formed from a polymer solution layer 1 mm thick (PU-1 mm) were porous with highly interconnected pores. The membranes formed from a polymer solution layer 2 mm thick were almost nonporous, and the membranes prepared from a 3 mm thick polymer solution layer (PU-3 mm) had a few open pores at the surfaces contacting both the glass substrate and the air.

4.6 Nonsolvent

The porous structures of the membranes obtained from the polymer solution in DMF with admixed water nonsolvent are shown in Fig. 5. The membranes' surface in contact with the air contained homogeneously distributed pores with sizes in the range of 5–20 μm. The surface in contact with the glass was microporous with pore sizes in the range of 1–5 μm. Laminated layers of longitudinally elongated interconnected pores were present in the membranes' cross-section.

4.7 Solid porogenes

In a previous study by one of the authors (Gogolewski), the use of sodium carboxymethylcellulose as a solid porogene for the preparation of experimental pericardial patches and membranes for guided tissue regeneration (GTR) was found to promote the development of micropores in the walls separating large pores and improving interaction with the tissues [6, 8, 12, 49]. The use of calcium L-lactate as a solid porogene for the preparation of microporous 3D polylactide scaffolds for the treatment of critical-size segmental bone defects, improved the homogeneity of pore structure [50]. In this study the presence of solid porogenes in the polyurethane solutions did not contribute to the porous structure of the membranes.

4.8 Water permeability

The results of water permeability measurements are shown in Fig. 6. The polyurethane membranes obtained from the polymer solutions in DMF and DMAC exhibited significantly higher water permeability (0.69 kg/s m^3 Pa for PU-DMF, and 0.54 kg/s m^3 Pa for PU-DMAC) than those obtained from the polymer solutions in DMSO (0.03 kg/s m^3 Pa) ($P < 0.0001$). The water permeability of the membranes formed from the polymer solution layers of the same thickness cast for 24–120 h was higher (0.63–0.72 kg/s m^3 Pa) than the permeability of the membranes cast for 8 h (0.36 kg/s m^3 Pa). The water permeability of the membranes formed from a 1 mm thick polymer solution layer (PU-1 mm) was significantly higher (0.69 kg/s m^3 Pa) than the membranes prepared from 2 mm (PU-2 mm) and 3 mm (PU-3 mm) thick polymer solution layers (0.11 kg/s m^3 Pa for PU-2 mm, and 0.08 kg/s m^3 Pa for PU-3 mm) ($P < 0.0001$). The water permeability of the membranes prepared from polymer solutions with concentrations of 2.5% and 5% (w/v) were higher (0.87 kg/s m^3 Pa for PU-2.5%, and 0.69 kg/s m^3 Pa for PU-5%) ($P < 0.005$) than the permeability of the membranes produced from polymer solutions with a concentration of 10% (w/v) (0.02 kg/s m^3 Pa) ($P < 0.0001$). The PU-NS membranes obtained from a 1 mm thick solution layer of the polyurethane in a mixture of DMF and nonsolvent (10:1), which were additionally sprayed with a nonsolvent after 24 h of setting, showed relatively high water permeability (0.68 ± 0.14 kg/s m^3 Pa). Water uptake by the membranes during the whole duration of a single test lasting 20 min was less than 0.1%.

4.9 Thermal analysis

The isosorbide-based polyurethane used in the study showed three low-energy thermal transitions at 78, 153 and 183°C which were assigned to the melting of the hard segments and/or melting of poorly organized crystals formed in the material upon casting [14, 15].

4.10 Tensile properties

The Young's modulus, stress at break and elongation at break of the microporous polyurethane membranes and the nonporous polyurethane foil (PU-REF) are listed in Table 2. Typical examples of load–displacement curves recorded for these samples are shown in Fig. 7. As it might be expected the tensile properties of the nonporous polyurethane foil were much higher than those of the microporous membranes. The tensile properties of the membranes cast from the polyurethane solutions in DMAC were inferior to those of the membranes cast from the polymer solution in DMF (PU-DMF-24 h, PU-DMF-48 h, PU-DMF-72 h, PU-DMF-NS). The PU-NS membranes showed an intermediate Young's modulus but the highest values for stress at break and elongation at break.

4.11 Suture pull-out test

The measured values for the suture pull-out strength of the microporous membranes are shown in Fig. 8. It was not possible to measure the pull-out strength for the control nonporous polyurethane reference foils (PU-REF) as the suture always broke before it cut through the foil. Therefore, the values given for PU-REF refer to the break

Table 2 Tensile properties of the microporous polyurethane membranes and the nonporous reference foil

Membrane	Young's modulus (MPa)	Stress at break (MPa)	Elongation (%)
PU-REF	121.13 ± 9.90	57.62 ± 4.20	1073.46 ± 45.57
PU-DMAC	0.82 ± 0.28	0.19 ± 0.08	49.62 ± 5.24
PU-DMF-24 h	22.34 ± 1.27	2.89 ± 0.31	183.15 ± 10.47
PU-DMF-48 h	17.66 ± 1.84	3.09 ± 0.16	221.42 ± 12.87
PU-DMF-72 h	27.85 ± 1.20	3.26 ± 0.33	182.17 ± 5.43
PU-NS	20.45 ± 0.86	3.89 ± 0.22	306.14 ± 18.48

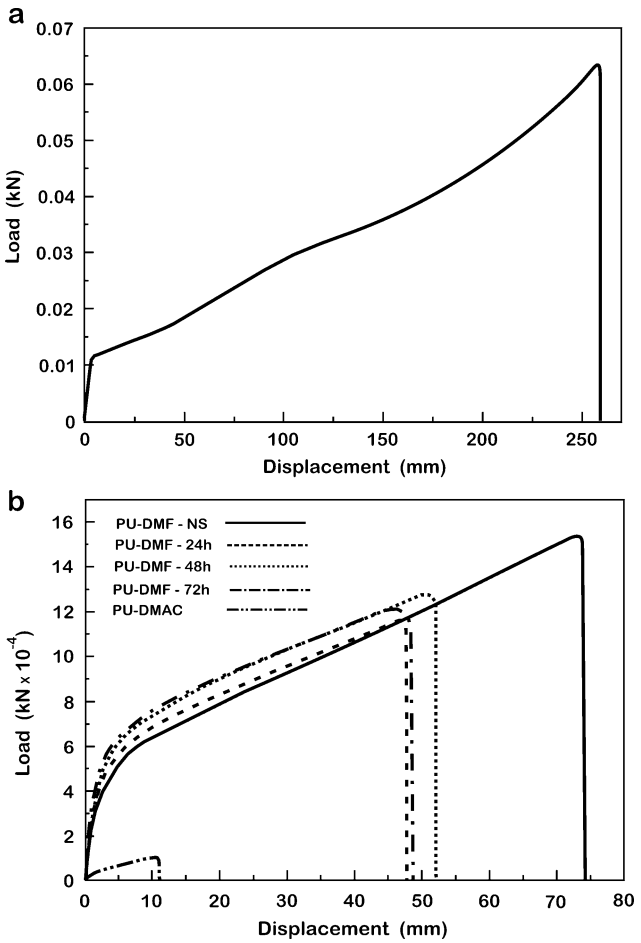

Fig. 7 Typical load–displacement curves for the polyurethane samples. **a** The nonporous foil cast from solution of the polyurethane in DMF; **b** various polyurethane membranes

strength (tensile load) required to break the suture. The pull-out strength for the PU-DMF-24 h and PU-DMF-48 membranes were similar ($P > 0.1$), while the PU-DMF-24 h and PU-DMF-48 h membranes showed significantly lower suture pull-out strength than PU-DMF-72 h membranes $P < 0.05$.

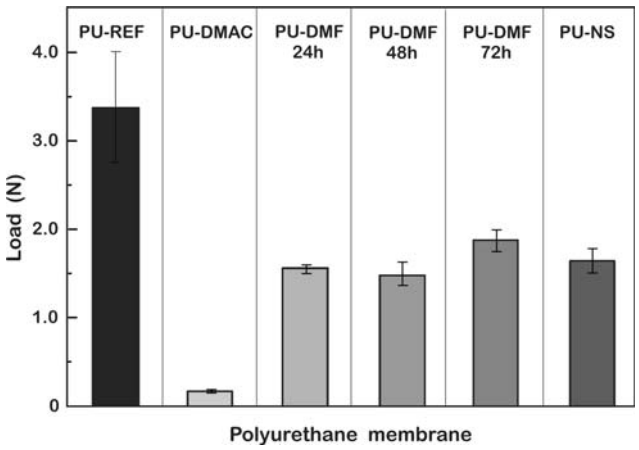

Fig. 8 Suture pull-out strength and/or suture break strength of the polyurethane samples. PU-REF, nonporous foil; PU-DMAC, porous membranes prepared from the polymer solution in dimethylacetamide (DMAC); PU-DMF-24 h; PU-DMF-48 h; PU-DMF-72 h and PU-NS, porous membranes prepared from the polymer solution in dimethylformamide (DMF) containing water as nonsolvent

5 Discussion

Polyurethanes are the materials of choice for a number of biomedical applications. The versatile chemistry of polyurethanes permits synthesis of biomaterials across a broad range of chemical, physical and biological properties. Polyurethanes can be produced as relatively biostable or as biodegradable materials. Covalent incorporation of various biologically active molecules in the backbone chain of polyurethanes designed for tissue engineering may promote the interaction of scaffolds from such materials with cells and tissues. Recently, an experimental biodegradable polyurethane has been developed based on biologically active 1,4:3,6-dianhydro-D-isosorbide [14, 15]. Three-dimensional porous scaffolds [15] from this aliphatic polyurethane supported attachment and proliferation of osteogenic cells and chondrocytes [16–19] in culture. Impregnation of these scaffolds with plant polyprenols and/or incorporating polyprenols in the polymer chain upon synthesis [21, 22] promoted attachment, proliferation and growth of cells [22]. Such 3D scaffolds might potentially be used as cancellous bone graft substitutes [23, 24] and, in the form of microporous membranes, for the treatment of articular cartilage defects [37, 38] and as skin wound covers.

In the published literature [39–47] the relationships between the conditions of fabrication and the morphology of the porous polymeric structures produced by the phase-inversion technique are usually explained by the concept of liquid–liquid demixing and solid–liquid demixing. Interdiffusion of the nonsolvent and the solvent brings the composition of the homogeneous polymer solution into the miscibility gap of the ternary phase diagram. Hence, the

polymer solution is decomposed into a polymer-rich phase and a polymer-poor phase. At a certain stage during phase demixing, the polymer-rich phase is solidified into a solid matrix, while the polymer-poor phase develops into the pores. The performance of such membranes depends largely on the morphology formed during phase separation and solidification.

In general, phase separation via liquid–liquid demixing prevails upon casting of polymer solutions with relatively low concentrations, and phase separation via solid–liquid demixing is typical for casting polymer solutions with higher concentrations.

While the porous structure formed in polymers via liquid–liquid demixing has cellular, interconnected pore morphology, the porous structures formed via solid–liquid demixing consist mainly of closed cell pores. The nascent pores which are developed upon liquid–liquid demixing are surrounded by the walls originating from the polymer-rich phase and in some cases can also be porous. This process continues until the polymer–solvent–nonsolvent system reaches thermodynamic equilibrium [40], which in turn depends on the solvent used for polymer dissolution, polymer concentration in solution, the type of nonsolvent and its miscibility with solvent and temperature.

Depending on the conditions of the phase-inversion process the porous structure formed will differ in pore size, structure, distribution and interconnectivity. The latter feature is of particular importance for porous scaffolds designed for tissue engineering as it allows for the ingrowth of cells, flux of nutrients and vascularization.

Although phase-inversion is a very flexible technique allowing porous polymer structures with various morphologies to be obtained, its main drawback relates to the fact that it is material specific. Hence, the conditions of the phase-inversion process have to be identified and individually tuned up for a given polymer to obtain reproducible porous structures with controllable morphology, pore-to-volume ratios and pore sizes.

This study aimed to define best conditions for the phase-inversion process for the preparation of isosorbide-based biodegradable polyurethane membranes with interconnected pores of controllable sizes and morphology suitable for tissue engineering. The factors affecting membranes' formation investigated in the study were the type of solvent used for polymer dissolution, the polymer concentration in solution, the admixed nonsolvent and/or solid porogene, the thickness of layer of polymer solution cast on a substrate and the time allowed for setting before the polymer gel was finally covered with a nonsolvent.

It has been found that solvent used for polymer dissolution plays a predominant role in the development of porous structure in the polyurethane membranes. Although all three solvents used, i.e. dimethylformamide (DMF), dimethylacetamide (DMAC) and dimethylsulfoxide (DMSO) were hydrogen-bonding liquids with comparable solubility parameters, only the membranes obtained from the polymer solutions in DMF and DMAC had a porous structure with interconnected pores, irrespective of the fact that in the given experiment all the cast solutions had the same polymer concentration and contained the same amount of nonsolvent. This might indicate that the appropriate conditions for liquid–liquid demixing were achieved in these two solvents, allowing for the simultaneous growth of pores in the polymer-poor phase and in the polymer-rich phase. These membranes and especially the ones prepared using DMAC as solvent showed the highest water permeability. Unfortunately, the membranes obtained from the polymer solutions in DMAC had poor mechanical properties, which make them less suitable for those applications where an implanted membrane would have to be sutured or subjected to tensile stress.

The polyurethane membranes prepared using DMSO as solvent had interconnected pores in the bulk and thin dense skin layers on the surfaces in contact with glass or air. This might be due to the fact that solubility of DMSO in water is higher than the water solubility of DMF and DMAC, which facilitated demixing of the ternary system and rapid phase-inversion. As both sides of the membranes formed from the polymer solutions in DMSO were microscopically nonporous, their water permeability was substantially reduced. Although membranes produced from the polymer solution in DMSO might potentially find other applications, e.g. as gas separation membranes, their use for tissue engineering seems less feasible.

The membranes' structure was also affected by the gelation time, i.e. the time allowed for solvent evaporation before the solidifying gel was treated with the coagulant. This effect was evaluated for the membranes produced from the 5% (w/v) polymer solution in DMF, and the solvent evaporation times were 8, 24, 48, 72, and 120 h.

The membranes that were given 8 h for setting were macroporous as the high amount of solvent remaining in the gel promoted continuous growth of pores in the bulk. The setting times of 24 and 48 h seemed to be optimal for the formation of membranes with bicontinuous porous structure. The original thickness of these membranes was retained as the setting times allowed for the relaxation of the tension generated in the polymer gel upon solvent evaporation. An increase of evaporation time to 72 and 120 h resulted in the formation of more compact, thinner membranes having a flattened air-contact surface. This may be due to the gravitational shrinkage of polymer in the direction perpendicular to the glass-contact surface [41].

The process of formation of porous polyurethane membranes and structure, size and morphology of pores was dependent on the thickness of cast solution layer [42].

Surprisingly, with increasing thickness of cast solution layer, the pore interconnectivity and pore distribution density in the bulk of the PU-2 mm and PU-3 mm membranes increased, but the surfaces of these membranes were less porous than the surface of PU-1 mm membranes. This was the reason why the water permeability of the PU-2 mm and PU-3 mm membranes was lower than that of the PU-1 mm membranes. It can be assumed that for a given concentration of the polymer solution, the larger solution volume (thicker solution layer) allows for the simultaneous formation of both the pores and the pore walls, and preservation of the original membrane thickness. In this set of experiments the membranes obtained using a cast solution layer with a thickness of 1 mm had the best porous structure.

Another factor which determines the formation of porous polymer structures by phase-inversion is the concentration of polymer in solution. It has been reported that the useful range of polymer concentration to produce such porous structures is narrow and does not exceed 20% [43–47]. Within this range, an increase of polymer concentration usually results in membranes having thicker surface layers, low porosity and interconnectivity of pores in the bulk, smaller pore size, and consequently lower permeability to water [42].

Furthermore, in this study, the polymer concentration in solution was found to significantly affect the structure of the polyurethane membranes. The membranes formed from polymer solutions with lowest concentration had two distinct porous layers. The surface layer was populated with irregular pores, while the membranes' bulk was filled with regular pores of uniform size. The optimal polymer concentration to produce membranes with bicontinuous porous structure was 5% (w/v). The membranes obtained from polymer solutions with highest concentration (10%, w/v) were filled with palisade-like pores. The low evaporation rate of the relatively large amount of nonvolatile solvent remaining in the polymer gel, allowed sufficient time for growth of the palisade-like macropores. Unfortunately, these membranes had a nonporous skin layer resulting in low water permeability.

In the present study the PU-NS membranes produced from polymer solutions with a concentration of 5% (w/v) in DMF containing admixed nonsolvent had the adequate mechanical properties and the best pore size and structure of all the membranes for the intended applications, i.e. for periosteal flap substitution or artificial skin. The presence of a nonsolvent seems to reduce the demixing time of the system [42] thus, promoting formation of interconnected pores in both the membrane bulk and the surface exposed to the air.

It is hypothesized that these polyurethane membranes might potentially be used as "an artificial periosteum" in the treatment of articular cartilage defects. The use of pliable elastomeric membranes withstanding high strain would avoid the implant fracture resulting from the shear forces acting at suture points and reduce severe tissue irritation which is often observed at the rigid implant–soft tissue interface.

In clinical practice, the surface of the membrane with open interconnected pores, which supports attachment and proliferation of cells, would be seeded with autogenous chondrocytes and placed towards the defect. The opposite side of the membrane with small-size micropores might act as a barrier to prevent fibrous tissue from invading the defect. The high permeability of the membranes might facilitate the diffusion of nutrients into the defect. The membranes withstand suturing irrespective of their highly porous interconnected structure. Such membranes seeded with autogenous keratinocytes might also be used in the treatment of full-thickness skin wounds.

6 Summary and conclusions

Microporous biodegradable polyurethane membranes were produced using a modified phase-inverse process. The structure, geometry and size of pores were controlled by selecting suitable solvents and nonsolvents, adjusting the polymer concentration in solution, and adjusting the volume of cast solution and the membrane setting time. The foreseen applications of the membranes are as an artificial periosteal flap in the treatment of articular cartilage defects and as skin wound covers. The biological functionality of the membranes can be promoted using a tissue engineering approach.

Acknowledgement One of the authors (Yuen Kee Tsui) thanks Ms. Katarzyna Gorna, PhD, for her help with polyurethane synthesis and DSC measurements.

References

1. Gogolewski S, Pennings AJ, Lommen E, Wildevuur CRH, Nieuwenhuis P. Growth of a neo-artery induced by a biodegradable polymeric vascular prosthesis. Makromol Chem Rapid Commun. 1983;4(4):213–9.
2. Gogolewski S, Pennings AJ. An artificial skin based on biodegradable mixtures of polylactides and polyurethanes for full thickness wound covering. Makromol Chem Rapid Commun. 1983;4(10):675–80.
3. Lipatova TE, Pkhakadze GA, Snegirev AI, Vorona VV, Shilov VV. Supermolecular organization of some polyurethanes containing sugar derivatives in the main chain. J Biomed Mater Res. 1984;18(2):129–36.
4. Gogolewski S, Galletti G. Degradable, microporous vascular prosthesis from segmented polyurethane. Colloid Polym Sci. 1986;264(10):854–8.
5. Gogolewski S, Galletti G, Ussia G. Polyurethane vascular prosthesis in pigs. Colloid Polym Sci. 1987;265(9):774–8.

6. Gogolewski S, Walpoth B, Rheiner P. Polyurethane microporous membranes as pericardial substitutes. Colloid Polymer Sci. 1987;265(11):971–7.
7. Gogolewski S. Selected topics in biomedical polyurethanes: a review. Colloid Polym Sci. 1998;267(9):757–85.
8. Walpoth BH, Rheiner P, Cox JN, Faidutti B, Megevand R, Gogolewski S. Implantations chroniques de membranes et prothèses en polyurethanes. Helv Chir Acta. 1988;55(1–2):157–62.
9. Farsø Nielsen F, Karring T, Gogolewski S. Healing of radial bone defects in rabbits using biodegradable membranes. J Dent Res. 1990;69:168–9.
10. Kostopoulos L, Karring T. Guided bone regeneration in mandibular defects in rats using a bioresorbable polymer. Clin Oral Implants Res. 1994;5(2):66–74.
11. Warrer K, Karring T, Nyman S, Gogolewski S. Guided tissue regeneration using biodegradable membranes of polylactic acid or polyurethane. J Clin Periodontol. 1992;19:633–40.
12. Farsø Nielsen F, Karring T, Gogolewski S. Biodegradable guide for bone regeneration Polyurethane membranes tested in rabbit radius defects. Acta Orthop Scand. 1992;63(1):66–9.
13. Atala A, Lanza RP, editors. Methods of tissue engineering. San Diego: Academic Press; 2001.
14. Gorna K, Gogolewski S. In vitro degradation of novel medical biodegradable aliphatic polyurethanes based on ε-caprolactone and Pluronics® with various hydrophilicities. Polym Degrad Stabil. 2002;75(1):113–22.
15. Gorna K, Gogolewski S. Porous biodegradable polyurethane scaffolds for tissue repair and regeneration. J Biomed Mater Res. 2006;79A(1):128–38.
16. Lee CR, Grad S, Gorna K, Gogolewski S, Goessl A, Alini M. Fibrin–polyurethane composites for articular cartilage tissue ngineering: A preliminary analysis. Tissue Eng. 2005;11(9–10):1562–73.
17. Chia SL, Gorna K, Gogolewski S, Alini M. Potential of elastomeric membranes from biodegradable polyurethanes as periosteal flap substitute: A preliminary in vitro evaluation. Tissue Eng. 2006;12(7):1945–53.
18. Chroscicka A, Tsui YK, Alini M, Gogolewski S. Differentiation of human mesenchymal stem cells on biodegradable polyurethane membranes for tissue engineering. In: Transactions of the 2006 annual meeting of the society for biomaterials, Pittsburgh, USA, p. 571, 2006, April 26–29.
19. Hill CM, An YH, Kang QK, Hartsock LA, Gogolewski S, Gorna K. Osteogenesis of osteoblast seeded polyurethane-hydroxyapatite scaffolds in nude mice. Macromol Symp. 2007;253:94–7.
20. Schlickewei C, Verrier S, Lippross S, Pearce S, Alini M, Gogolewski S. Interaction of sheep bone marrow stromal cells with biodegradable polyurethane bone substitutes. Macromol Symp. 2007;253:162–71.
21. Gogolewski S. Biomedical polymer material for tissue repair and engineering. WO2008017170-A1; 2008.
22. Walinska K, Iwan A, Gorna K, Gogolewski S. The use of long-chain plant polyprenols as a means to modify biological properties of new biodegradable polyurethane scaffolds for tissue engineering. A pilot study. J Mater Sci: Mater Med. 2008;19:129–35.
23. Gogolewski S, Gorna K, Turner AS. Regeneration of bicortical defects in the iliac crest of estrogen-deficient sheep, using new biodegradable polyurethane bone graft substitutes. J Biomed Mater Res. 2006;77A(4):802–10.
24. Gogolewski S, Gorna K. Biodegradable polyurethane cancellous bone graft substitutes in the treatment of iliac crest defects. J Biomed Mater Res. 2007;80A(1):94–101.
25. Guan JJ, Fujimoto KL, Sacks MS, Wagner WR. Preparation and characterization of highly porous, biodegradable polyurethane scaffolds for soft tissue applications. Biomaterials. 2005;26(18):3961–71.
26. dal Prà P, Petrini A, Charini S, Bozzini S, Farè S, Armato U. Silk fibroin-coated three-dimensional polyurethane scaffolds for tissue engineering: interactions with normal human fibroblasts. Tissue Eng. 2003;9(6):1113–21.
27. Siepe M, Giraud MN, Liljensten E, Nydegger U, Menasche P, Carrel T, et al. Construction of skeletal myoblast-based polyurethane scaffolds for myocardial repair. Artif Organs. 2007;31(6):425–33.
28. Hafeman AE, Li B, Yoshii T, Zienkiewicz K, Davidson JM, Guelcher SA. Injectable biodegradable polyurethane scaffolds with release of platelet-derived growth factor for tissue repair and regeneration. Pharmaceutical Res. 2008;25(10):2387–99.
29. Ramarattan NN, Heikants RGJC, van Tienen TG, Schouten AJ, Veth RPH, Buma P. Assessment of tissue ingrowth rates in polyurethane scaffolds for tissue engineering. Tissue Eng. 2005;11(7–8):1212–23.
30. Zhu YB, Gao CY, Guan JJ, Shen JC. Engineering porous polyurethane scaffolds by photografting polymerization of methacrylic acid for improved endothelial cell compatibility. J Biomed Mater Res. 2003;67A(4):1367–73.
31. Zhang JY, Doll BA, Beckman EJ, Hollinger JO. A biodegradable polyurethane-ascorbic acid scaffold for bone tissue engineering. J Biomed Mater Res. 2003;67A(2):389–400.
32. Guelcher SA, Patel V, Gallagher KM, Connolly S, Didier JE, Doctor JS, et al. Synthesis and in vitro biocompatibility of injectable polyurethane foam scaffolds. Tissue Eng. 2006;12(5):1247–59.
33. Borkenhagen M, Stoll RC, Neuenschwander P, Suter UE P, Aebischer P. In vivo performance of a new biodegradable polyester urethane system used as a nerve guidance channel. Biomaterials. 1998;19(23):2155–65.
34. Van Tienen TG, Heikants RGJC, Buma AP, De Groot JH, Pennings AJ, Veth RPH. Tissue ingrowth and degradation of two biodegradable porous polymers with different porosities and pore sizes. Biomaterials. 2002;23(8):1731–8.
35. McDevitt TC, Woodhouse KA, Hauschka SD, Murry CE, Stayton PS. Spatially organized layers of cardiomyocytes on biodegradable polyurethane films for myocardial repair. J Biomed Mater Res. 2003;66A(3):586–95.
36. Zhu YB, Gao CY, He T, Shen JC. Endothelium regeneration on luminal surface of polyurethane vascular scaffold modified with diamine and covalently grafted with gelatin. Biomaterials. 2004;25(3):423–30.
37. Brittberg M, Lindahl A, Nilsson A, Ohlsson C, Isaksson O, Peterson L. Treatment of deep cartilage defects in the knee with autologous chondrocyte transplantation. N Engl J Med. 1994;331(14):889–95.
38. Peterson L, Minas T, Brittberg M, Lindahl A. Treatment of osteochondritis dissecans of the knee with autologous chondrocyte transplantation. J Bone Joint Surg Am. 2003;85-A Suppl 2:17–24.
39. Klempner D, Frisch KC. The handbook of polymeric foams and foam technology. Munich, Germany: Hauser; 1991.
40. Mulder MHV. Basic principles of membrane technology. Dordrecht, Holland: Kluwer; 1991.
41. Kesting RE, Fritzsche AK. Polymeric gas separation membranes. New York: Wiley; 1993.
42. Strathmann H. Production of microporous media by phase inversion processes. In: Lloyd DR, editor. Materials science of synthetic membranes. Washington, DC: American Chemical Society; 1985. p. 165–95.
43. Strathmann H. Synthetic membranes and their preparation. In: Porter MC, editor. Handbook of industrial membrane technology. Park Ridge, NJ: Noyes; 1990. p. 1–26.

44. Laxminarayan A, Caneba GT. Analysis of polymer membrane formation through spinodal decomposition. II: Effect of Flory-Huggins enthalpic and entropic contributions. Polym Eng Sci. 1957;31(22):1597–603.
45. Van de Witte P, Dijkstra PJ, Van den Berg JWA, Feijen J. Phase separation processes in polymer solutions in relation to membrane formation. J Membr Sci. 1996;117(1–2):1–31.
46. Koenhen DM, Mulder MHV, Smolders CA. Phase separation phenomena during the formation of asymmetric membranes. J Appl Polym Sci. 1997;21(1):199–215.
47. Mikos AG, Temenoff JS. Formation of highly porous biodegradable scaffolds for tissue engineering. Electronic J Biotechnol. 2000;3(2):114–9.
48. Wright Medical Technology Brochure: SK 103–303; Rev. 09.04: 2004.
49. Farsø-Nielsen F, Karring T, Gogolewski S. Healing of radial bone defects in rabbits using biodegradable polyurethane membranes. In: Proceedings of the IADR/AADR conference, Cincinnati, USA, p. 16, 1990, Sept 3–5.
50. Gogolewski S, Rahn B, Wieling R. Bone regeneration in critical-size segmental defects in the tibiae using bioresorbable polymeric bone substitute. Proceedings of the 17th annual meeting of the Orthopaedic Trauma Association, San Diego, USA, p. 218–219, 2001, Oct 18–20.